Article

Sialic Acid as a Biomarker Studied in Breast Cancer Cell Lines In Vitro Using Fluorescent Molecularly Imprinted Polymers

Zahra El-Schich [1,2], Yuecheng Zhang [1,2], Tommy Göransson [1], Nishtman Dizeyi [3], Jenny L. Persson [1,2,4], Emil Johansson [5,6], Remi Caraballo [5,6], Mikael Elofsson [5,6], Sudhirkumar Shinde [7], Börje Sellergren [1,2] and Anette Gjörloff Wingren [1,2,*]

1   Department of Biomedical Sciences, Faculty of Health and Society, Malmö University, SE-205 06 Malmö, Sweden; zahra.el-schich@mau.se (Z.E.-S.); yuecheng.zhang@mau.se (Y.Z.); tommy.goransson@skane.se (T.G.); jenny.persson@mau.se (J.L.P.); borje.sellergren@mau.se (B.S.)
2   Biofilms-Research Center for Biointerfaces, Malmö University, SE-205 06 Malmö, Sweden
3   Department of Translational Medicine, Lund University, SE-205 06 Malmö, Sweden; nishtman.dizeyi@cernelle.se
4   Department of Molecular Biology, Umeå University, 901 87 Umeå, Sweden
5   Department of Chemistry, Umeå University, 901 87 Umeå, Sweden; emil.johansson@umu.se (E.J.); remi.caraballo@umu.se (R.C.); mikael.elofsson@umu.se (M.E.)
6   Umeå Centre for Microbial Research, Umeå University, 901 87 Umeå, Sweden
7   School of Consciousness, Vishwanath Karad Maharashtra Institute of Technology—World Peace University, Kothrud, Pune 411038, India; sudhirkumar.shinde@mitwpu.edu.in
*   Correspondence: anette.gjorloff-wingren@mau.se

Abstract: Sialylations are post-translational modifications of proteins and lipids that play important roles in many cellular events, including cell-cell interactions, proliferation, and migration. Tumor cells express high levels of sialic acid (SA), which are often associated with the increased invasive potential in clinical tumors, correlating with poor prognosis. To overcome the lack of natural SA-receptors, such as antibodies and lectins with high enough specificity and sensitivity, we have used molecularly imprinted polymers (MIPs), or "plastic antibodies", as nanoprobes. Because high expression of epithelial cell adhesion molecule (EpCAM) in primary tumors is often associated with proliferation and a more aggressive phenotype, the expression of EpCAM and CD44 was initially analyzed. The SA-MIPs were used for the detection of SA on the cell surface of breast cancer cells. Lectins that specifically bind to the a-2,3 SA and a-2,6 SA variants were used for analysis of SA expression, with both flow cytometry and confocal microscopy. Here we show a correlation of EpCAM and SA expression when using the SA-MIPs for detection of SA. We also demonstrate the binding pattern of the SA-MIPs on the breast cancer cell lines using confocal microscopy. Pre-incubation of the SA-MIPs with SA-derivatives as inhibitors could reduce the binding of the SA-MIPs to the tumor cells, indicating the specificity of the SA-MIPs. In conclusion, the SA-MIPs may be a new powerful tool in the diagnostic analysis of breast cancer cells.

Keywords: breast cancer; epithelial cell adhesion molecule; molecularly imprinted polymers; nanoparticles; sialic acid

1. Introduction

Breast cancer cannot be classified as one diseases, but is largely heterogeneous and therefore the diagnosis and treatment in affected women with breast cancer can vary. Although there is a recent improvement in overall survival rate, the mortality rate is high [1]. Proved by molecular profiling, breast cancer is comprised of several subgroups according to previous classification: luminal A, luminal B, basal-like, human epidermal growth factor receptor 2 (HER2)-positive and normal subgroups [2,3].

Cancer cells use several mechanisms to bypass recognition by the immune cells, thereby escaping immune surveillance and progressing through metastases [4]. The cir-

culating tumor cells (CTCs) released from primary tumors are considered to have the capability to initiate distant metastasis. Detection and isolation of CTCs using the Food and Drug Administration (FDA)-approved CellSearch platform is based on automated immunomagnetic sorting and on expression of the epithelial cell adhesion molecule (EpCAM) and cytokeratin [5]. The expression of EpCAM in primary tumors is often associated with proliferation and a more aggressive phenotype, if it is considered as high [6]. Alternative methods are definitely needed for the detection of CTCs that are able to recognize a broader spectrum of phenotypes.

Alterations in protein glycosylation have a role in the transformation to cellular malignancy and cancer progression [7]. Sialic acid (SA), or 5-N-acetylneuraminic acid (Neu5Ac), is a monosaccharide that plays an important role in many biological processes in the cells [8]. SA is chemically bound to galactose (Gal) or N-acetylgalactosamine (GalNAc) and the underlying glycan via α-2,3 or α-2,6 glycosidic linkage [8]. For detection of α-2,3 SA, the lectin *Maackia amurensis* I (MAL I) is commonly used, and for detection of α-2,6 SA, the lectin *Sambucus nigra* (SNA) is used. α-2,6-SA can be found on the basolateral cell membrane, whereas α-2,3-SA seems to be more prominent on the apical cell membrane [9].

Increased levels of SA on tumor cells have been connected with poor prognosis of clinical tumors and increased invasive potential [10]. It has been shown that a high SA expression enhances migration and invasion by increasing integrin interaction and preventing immune cell recognition [11]. The upregulation of sialyltransferase expression is upregulated and results in the accumulation of SA on the surface of cells [12,13].

Available lectins and glycan specific antibodies for detection of SA containing glycoconjugates do not perform well in, e.g., analytics of glycoproteomes and appropriate high-throughput cellular imaging technologies [14]. Therefore, the studies by us and others are of high importance to develop novel tools for glycan detection [15–17]. One such tool to prepare saccharide selective receptors is molecular imprinting [18]. Since Wulffs early reports on highly discriminative boronate-based receptors for monosaccharides [19], new promising imprinting approaches to design glycan or glycoprotein specific probes have been reported [20–27]. Indeed, the design of molecularly imprinted polymers (MIPs) and their use as artificial recognition elements have been shown to be successful for targeting glycans such as SA and glycosamino-glycans (GAGs) [15].

Liu et al. have reported, in a series of publications, an orientation controlled imprinting procedure using boronate anchored glycans [25]. This has resulted in glycan specific nanoprobes showing high selectivity for cell surface glycosylations. Using an innovative multilayered core-shell architecture comprising quantum dot cores, nanoprobes were developed for selective targeting and imaging of hyaluronan and sialylated glycosylation sites on human keratinocytes [22]. Based on a ternary complex imprinting procedure, we recently reported on fluorescently reporting SA imprinted nanoprobes for combined detection of both α-2,3 and α-2,6 SA on cancer cells. We demonstrated an affinity for various cell lines such as DU145, PC-3, Jurkat, and B-CLL and further verified the binding specificity by enzymatic cleavage of fluorescent SA-MIP nanoprobes for detection of SA on cancer cells [20,21].

In the present study, we have performed screening of SA expression on a collection of breast cancer cell lines by using SA-MIPs and lectins, and analyzed SA-MIP targeting to the cells by flow cytometry and confocal fluorescence microscopy. The breast cancer cell lines were also analyzed using antibodies for the expression of the epithelial EpCAM and CD44, which is overexpressed in several cell types including cancer stem cells. We show that the SA-MIPs recognize breast cancer cells with low CD44 and high EpCAM expression, indicating that SA-MIPs can be used as an additional tool for detecting EpCAM positive breast cancer cells. The fluorescence microscopy images revealed the staining pattern of both lectins and SA-MIPs. Importantly, we show a novel use for SA-derivatives by pre-treating the SA-MIPs with these inhibitors before cell staining. Thereby, we could demonstrate a concentration-dependent reduction in binding of the SA-MIPs to breast cancer cells, indicating the specificity of the SA-MIP interaction.

2. Materials and Methods

2.1. Cell Culture

Human breast cancer cell lines T47D, MCF-7, Cama-1, MDAMB468, MDAMB231, and Hs-578T were obtained from the American Type Culture Collection (ATCC/LGC Standards, Teddington, UK). T47D and MCF-7 cells were cultured in Roswell Park Memorial Institute - 1640 (RPMI-1640) medium supplemented with 10% fetal bovine serum (FBS) and 50 ug/mL gentamycin. MDAMB468 and MDAMB231 cells were cultured in Dulbeccos Modified Eagle Medium (DMEM), supplemented with 10% FBS. Cama-1 cells was cultured in RPMI-1640 medium supplemented with 10% FBS, 1% pyruvate sodium, and 1% penicillin streptomycin. Hs-578T cells was cultured in DMEM supplemented with 10% FBS, 1% penicillin streptomycin, and 10 ug/mL insulin (Sigma–Aldrich, St Louis, MO, USA). The cell lines were incubated at 37 °C with 5% CO_2 in 100% humidity. All cell culture reagents, except for insulin, were from Thermo Fisher Scientific, Waltham, MA, USA).

2.2. Flow Cytometry Analysis

EpCAM staining: 1×10^6 cells/sample were stained with anti-EpCAM-PE, according to the manufacturer's instructions (Milentyi Biotec GmBH, Bergisch Gladbach, Germany) or left unstained as a control. The cells were washed twice with 2 mL phosphate-buffered saline (PBS, Thermo Fisher Scientific). Anti-EpCAM-PE (100 μL) with concentrations of 100, 50, and 10 ng/mL was added to the cells, and 100 μL of PBS was used as a negative control. The cells were incubated with EpCAM-PE for 30 min at 4 °C in the dark and were thereafter washed three times with 2 mL PBS and analyzed using flow cytometry (BD Biosciences, Accuri C6 Flow Cytometry, NJ, USA).

CD44 staining: 1×10^6 cells/sample were stained with human anti-CD44 antibody, according to the manufacturer's instructions (R&D, Minneapolis, MN, USA) or left unstained as a control. The cells were washed twice with 2 mL PBS. Anti-CD44 (100 μL) with a concentration of 2.5 μg/mL was added to the cells, and 100 μL of PBS was used as a negative control and incubated for 30 min at 4 °C in the dark. After incubation, the cells were washed twice with 2 mL PBS. Anti-rat fluorescein isothiocyanate (FITC, R&D) was used as a secondary antibody. Anti-rat-FITC (100 μL of 1:10 diluted) was added to the cells and to the negative control. The cells were incubated for 30 min at 4 °C in the dark and were thereafter washed three times with 2 mL PBS and analyzed using flow cytometry.

MAL I and SNA (Lectin-Biotin): 1×10^6 cells/sample were stained with Lectin-Biotin, according to the manufacturer's instructions (Vector Laboratories, Burlingame, CA, USA) both for MAL I and SNA or left unstained as a control. The cells were washed twice with 2 mL PBS. Lectin-Biotin (100 μL) with concentrations of 5, 2, and 1 μg/mL was added to the cells, and 100 μL of PBS was used as a negative control. The cells were incubated with Lectin-Biotin for 30 min at 4 °C and were thereafter washed three times with 2 mL PBS. Thereafter, 100 μL of 1:100 dilutions of streptavidin-FITC (Sigma) was added to the cells and incubated for 20 min at 4 °C in the dark. After the incubation, the cells were washed three times with 2 mL PBS and analyzed using flow cytometry.

SA-MIPs: The polymer particles (SA-MIPs) were prepared as previously described by Shinde et al. [20]. SA-MIPs equipped with nitrobenzoxadiazole (NBD) fluorescent reporter groups allowing environmentally sensitive fluorescence detection in green fluorescence. Here, 1×10^6 cells/sample were stained with SA-MIPs or left unstained as a control. The cells were washed twice with 2 mL PBS. SA-MIPs (100 μL) with a concentration of 0.1 mg/mL was added to the cells, and 100 μL of PBS was used as a negative control. The cells were incubated with SA-MIP for 30 min at 4 °C and were thereafter washed three times with 2 mL PBS and analyzed using flow cytometry.

2.3. Fluorescence Microscopy

Cells/sample (5×10^4) were adhered to poly-lysine slides (Thermo Fisher Scientific) in a 6 well-plate for 2 h at 37 °C with 5% CO_2 in 100% humidity. After the incubation, 2 mL cell culture medium was added to the wells and incubated for 48 h. After the incubation,

the cells were washed three times with PBS and fixed with 100 μL 4% formaldehyde for 10 min, followed by washing three times with PBS. After permeabilization with 0.05% TritonX (Sigma) the cells were incubated with rhodamine-Phalloidin (Sigma) for 30 min in the dark at room temperature (RT). After two more washings with 0.05% Triton-X and PBS, the cells were incubated with 100 μL of SA-MIPs (0.1 mg/mL) or biotinylated MAL I and SNA (10 μg/mL) for 30 min at RT. The biotinylated lectins were further incubated with streptavidin-FITC. After the incubation, the cells were washed four times with PBS and incubated with 100 μL 300 nM 4′,6-diamidino-2-phenylindole (DAPI, Thermo Fisher Scientific) in PBS, for 4 min at RT. After three more washes with PBS, the cells were mounted with one drop of mounting medium ProlongQR Gold antifade reagent (Molecular probes).

Pre-treatment of SA-MIPs with SA- derivatives: The cells were harvested and washed twice with 2 mL PBS. SA-MIPs and two different SA-derivatives (ME0970 and ME1057) [28] at either 20 μM or 200 μM in 100 μL were pre-incubated in PBS for 5 min before being added to 1×10^6 cells/sample, or were left unstained as a control. In addition, 100 μL of SA-MIPs with a concentration of 0.1 mg/mL was used as a positive staining control. The cells were incubated for 30 min at 4 °C and were thereafter washed three times with 2 mL PBS and analyzed using flow cytometry.

3. Results

3.1. Expression of EpCAM and CD44 on Breast Cancer Cell Lines

The expression levels of EpCAM were analyzed in the six different breast cancer cell lines. Hs-578T and MDAMB231 expressed no EpCAM compared to MDAMB468, T47D, Cama-1, and MCF-7, which all expressed EpCAM at higher levels (Figure 1A). For CD44 expression, the Hs-578T, MDAMB231, and MDAMB468 expressed CD44 at high levels compared to T47D, Cama-1, and MCF-7, which expressed CD44 at lower levels (Figure 1B).

3.2. SA Staining With Lectins on Breast Cancer Cell Lines

In this study, two different lectins were used and analyzed by flow cytometry and fluorescence microscopy. MAL I appear to bind carbohydrate structures that contain SA attached to terminal galactose in α-2,3 linkage. The α-2,3-SA expression is presented in Figure 2A. T47D, MDAMB231, and MCF-7 expressed high α-2,3 linkage levels compared to Cama-1 and Hs-578T, which expressed low levels of α-2,3 linkage, as determined by the mean fluorescence intensity (MFI). SNA binds preferentially to SA attached to terminal galactose in α-2,6 and, to a lesser degree, α-2,3 linkage. The α-2,6-SA expression is presented in Figure 2B. T47D and MDAMB468 showed the highest α-2,6 linkage levels compared to MCF-7 and Hs-578T, which showed low levels of α-2,6 linkage. The fluorescent microscopy results correlate well with the flow cytometry results (Figure 3).
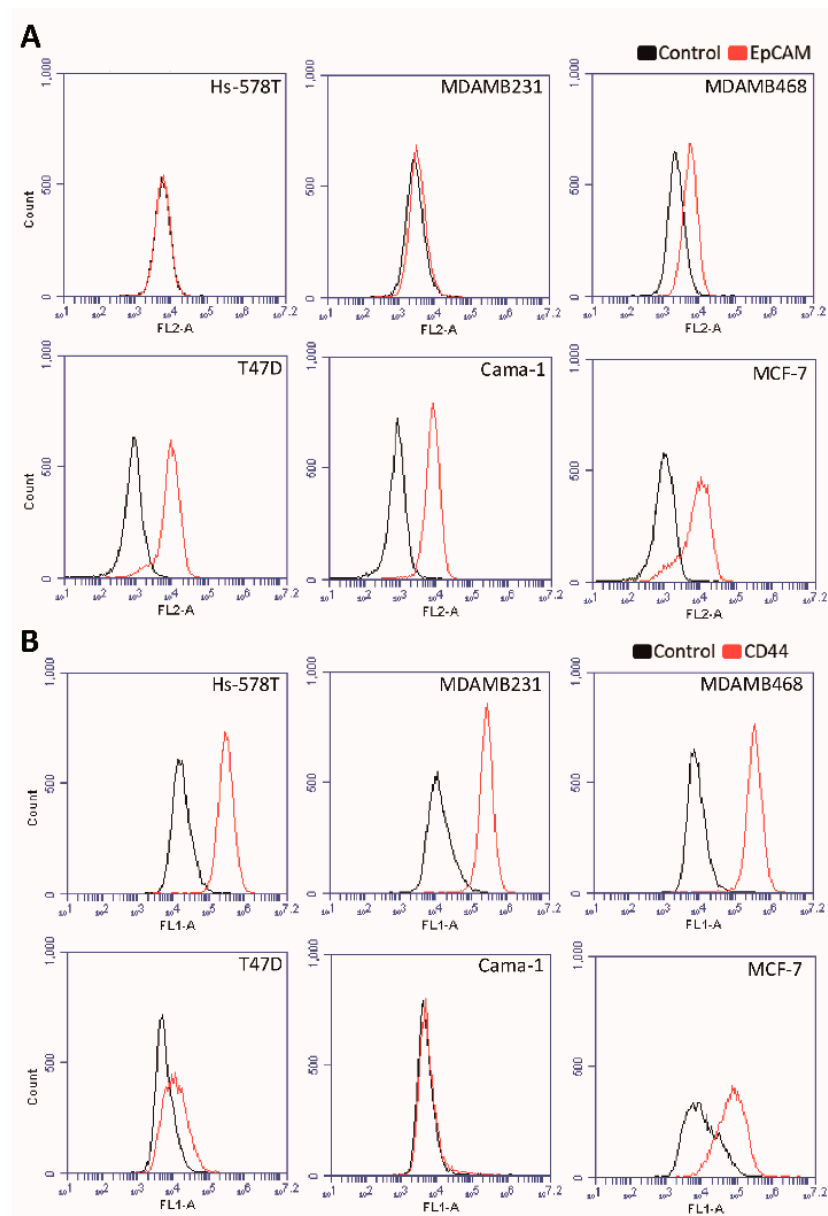
Figure 1. Epithelial cell adhesion molecule (EpCAM) and CD44 expression was analyzed with flow cytometry. Six different breast cancer cell lines were analyzed for EpCAM (**A**) and CD44 (**B**) expression patterns. The histograms shows the mean fluorescence intensity (MFI) for each staining in red, including background control in black.
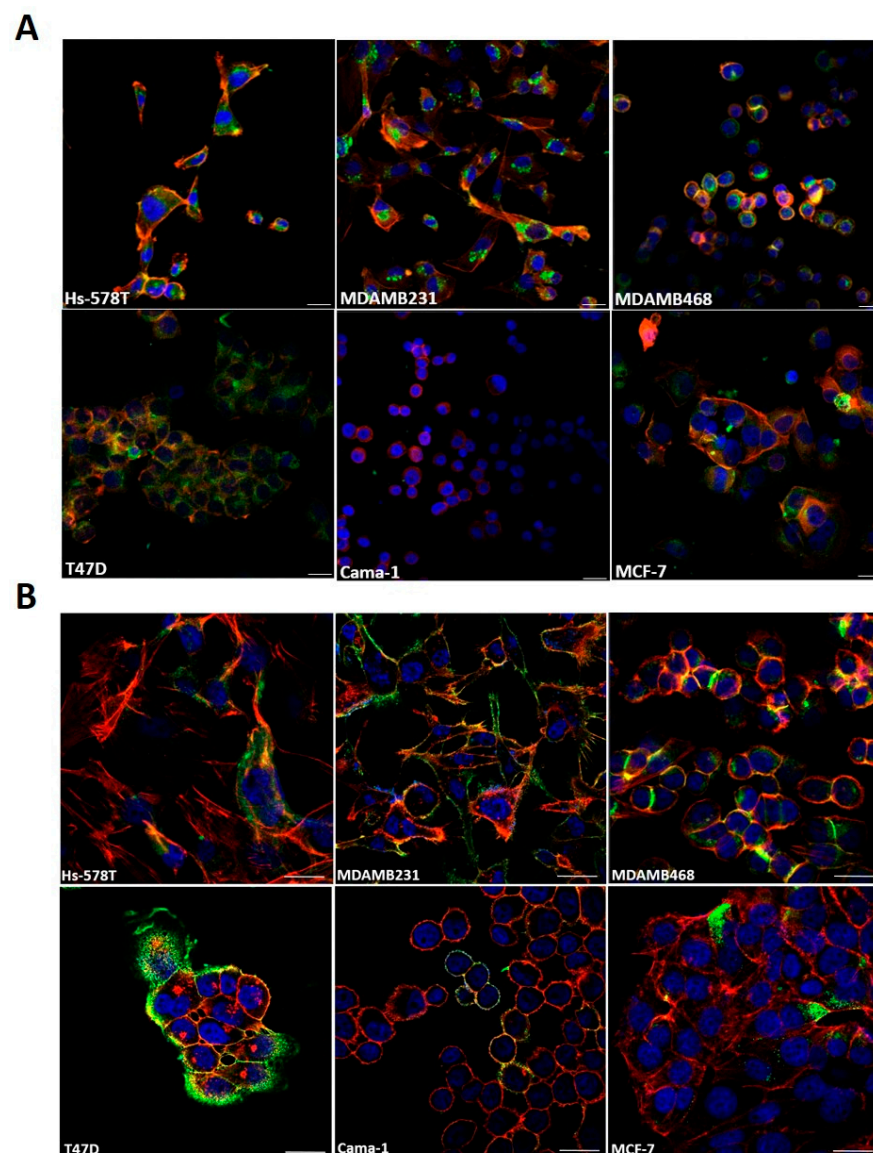
Figure 2. Fluorescence confocal microscopy of *Maackia amurensis* I (MAL I)—scale bar 20 μm. Six different breast cancer cell lines were stained for MAL I using fluorescein isothiocyanate (FITC, green), actin filament using rhodamine-phalloidin (red), and 4′,6-diamidino-2-phenylindole (DAPI) nuclear staining (in blue), and analyzed with fluorescence confocal microscopy (**A**). Fluorescence microscopy of *Sambucus nigra* (SNA)—scale bar 10 μm. Six different breast cancer cell lines were stained for SNA in green, actin filament in red, and nuclear in blue, and analyzed with fluorescence confocal microscopy (**B**).

3.3. SA Staining with SA-MIPs on Breast Cancer Cell Lines

The expression levels for SA were analyzed using SA-MIPs and flow cytometry in six different breast cancer cell lines. According to the binding pattern, Hs-578T and MDAMB231 expressed SA at low levels compared to MDAMB468, T47D, Cama-1, and MCF-7, which expressed SA at higher levels (Figure 4A). Interestingly, the results indicate that low EpCAM expression levels correlate with low SA expression levels (Figure 4B). In addition, there is an inverse correlation between SA- and CD44-expression. In order to visualize the surface binding of SA, breast cancer cell lines were stained with SA-MIPs and analyzed with fluorescent microscopy. In Figure 5, the membrane staining of the breast cancer cell lines using SA-MIPs, actin filament staining with rhodamine-phalloidin, and nuclei staining using DAPI is shown.
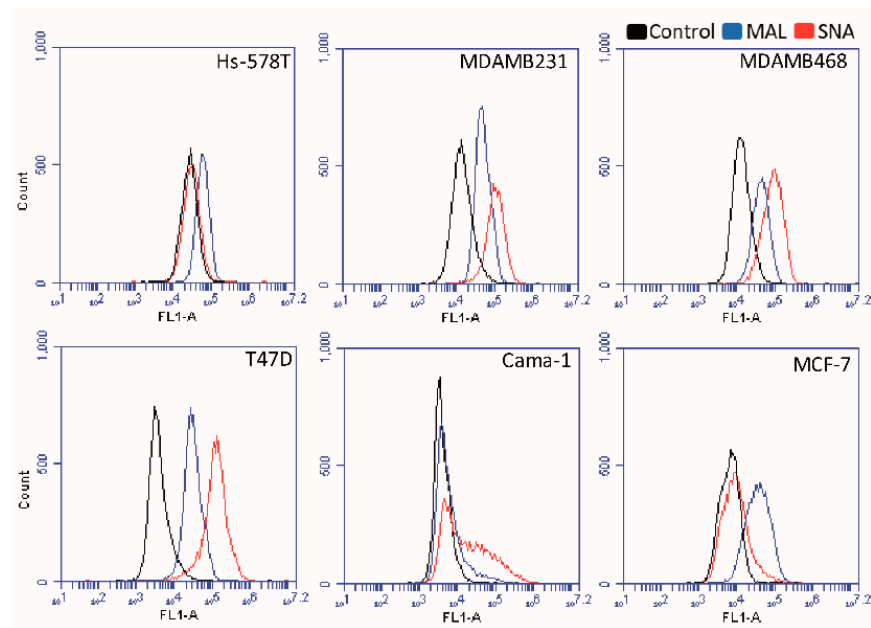
Figure 3. Six breast cancer cell lines were stained with either MAL I or SNA and analyzed with flow cytometry. The histograms show the MFI for each staining, MAL I in blue, SNA in red including background control in black.
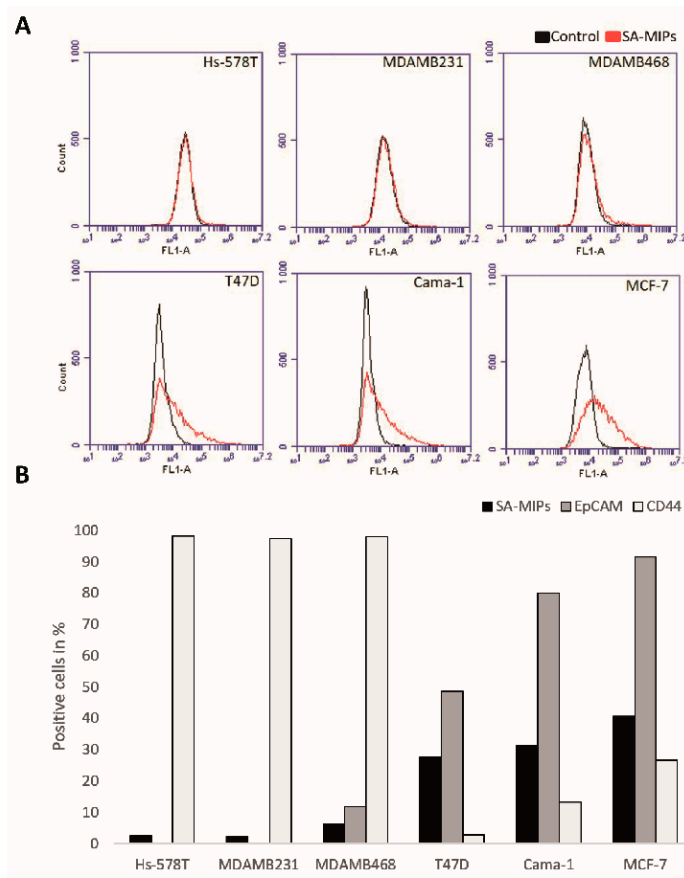

Figure 4. Six breast cancer cell lines were stained with SA-MIPs and analyzed with flow cytometry. The histograms shows the MFI for each staining, SA-MIPs in red including background control in black (**A**). EpCAM, CD44, and SA-MIPs analyzed with flow cytometry. Six different breast cancer cell lines were analyzed for EpCAM, CD44, and SA expression patterns. Results are shown in % positive cells (**B**).
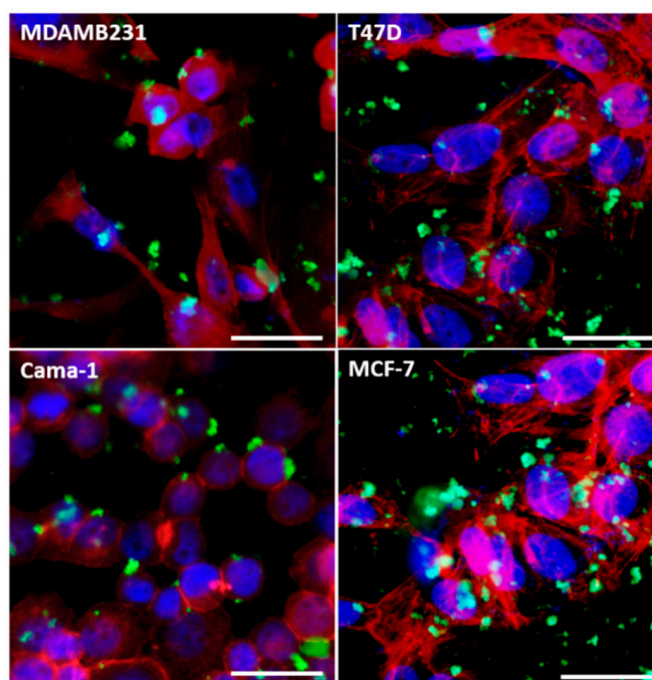
Figure 5. Fluorescence confocal microscopy SA-MIPs—scale bar 20 μm. Four different breast cancer cell lines were stained with SA-MIPs using nitrobenzoxadiazole (NBD) in green, rhodamine-phalloidin (actin filaments) in red, and DAPI (nuclei) in blue, and analyzed with fluorescence confocal microscopy.

3.4. Pre-Treatment of SA-MIPs with SA-Derivative Reduce the Binding to Cells

The SA-derivatives ME0970 or ME1057 were pre-incubated at either 20 μM or 200 μM, respectively, with 0.1 mg/mL SA-MIPs and were then added to the T47D cells. The binding of the pre-treated cells was compared with the binding to the same cell line of 0.1 mg/mL of SA-MIPs alone, and was shown to be reduced by 7% (20 μM) and 66% (200 μM), respectively, for ME0970, and by 0.5% (20 μM) and 64% (200 μM), respectively, for ME1057 (Figure 6). The reduction in binding of the pre-treated cells was concentration-dependent, as shown with both SA-derivatives.
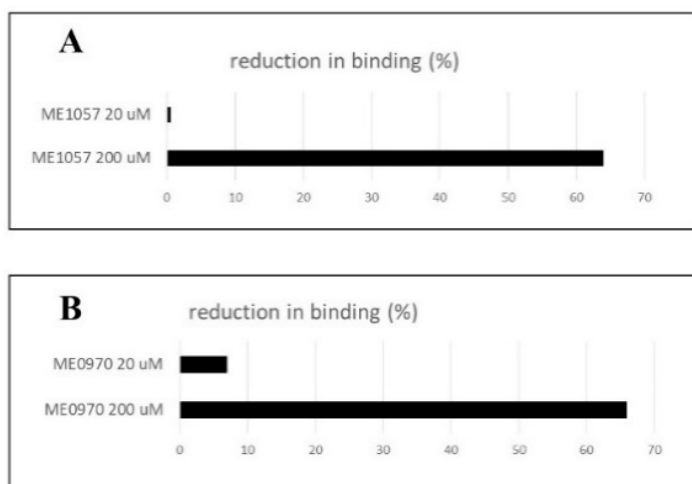

Figure 6. SA-MIPs were pre-incubated with different concentrations of the SA-derivatives and analyzed with flow cytometry. The reduction of binding compared to SA-MIP binding alone is shown. (**A**) The SA-derivative ME1057 was added at 20 μM and 200 μM. (**B**) ME0970 was added at 20 μM and 200 μM.

4. Discussion

Glycosylation is the most abundant post-translational modification, and the majority of eukaryotic cells express cell surface glycans [29]. Knowledge about glycome has increased in the past few years. Indeed, the role of glycans in cancer have been highlighted by the fact that alterations in glycosylation regulate the development and progression of cancer. Thus, glycans serve as important biomarkers. We have developed SA-imprinted fluorescent nanoprobes to enable SA-detection, for use as novel tools in cancer diagnostics [20]. The correlation of SA-MIP binding and EpCAM expression on the breast cancer cell lines presented in this study show an additive level of phenotyping of breast cancer cells, together with the CD44 biomarker, which showed a reverse correlation. High expression levels of EpCAM in tumors are often associated with proliferation and a more aggressive phenotype with respect to overall survival and appearance of metastasis [6]. Identification of EpCAM glycosylation sites or structures may be a crucial step to define the potential role of EpCAM in breast cancer cells [30]. Various cancer cells are lacking EpCAM expression, therefore CellSearch approaches are limited [31]. Indeed, carcinoma cells undergoing epithelial-to-mesenchymal transition can at least partially downregulate epithelial cell–specific molecules such as EpCAM [32]. Several glycosylated markers could be of interest for study, including CD24, a highly glycosylated mucin-like antigen that has recently emerged as a novel oncogene and metastasis promoter in breast carcinoma [33].

Our results show that breast cancer cells expressing α-2,3 or α-2,6 glycosidic linkage can bind the SA-MIPs to various degrees. The fluorescence confocal microscopy results show the binding pattern of the SA-MIPs to the different cell types. For flow cytometry analysis, we could characterize the binding pattern of MAL I, SNA, and SA-MIPs to all six cell lines. In order to validate that binding of the MIPs to cells is mediated by direct interaction with SA, the MIPs were pre-incubated with pentavalent SA-derivatives. These derivatives were designed to block attachment of coxsackievirus A24V and adenovirus 37 viruses to host cells [28]. The viruses use multivalent attachment, and these defined SA-derivatives are efficacious in cell based infection and attachment assays in contrast to the SA monosaccharide that need to be used in mM concentrations to observe week inhibition. We hypothesized that these derivatives, with their flexible and long spacers, should be capable of binding to the MIPs and thereby reduce cell binding. Indeed, the results showed that the binding of the SA-MIPs to the cell line T47D could be inhibited by the addition of two different SA-derivatives. Because of their efficient inhibition ability, SA-derivatives can be used for specificity tests for SA-MIPs. The two SA-derivatives used in this study were designed from multivalent ligands intended for topical administration for the viruses CVA24v and HAdV-37 that utilize SA for cell attachment [28].

Others have shown that SA-imprinted nanoparticles could selectively bind with the SA overexpressed in DU145 cancer cells [25]. In their hands, DU145 cells, but not HeLa cells, bound the SA-imprinted nanoparticles, revealing a specificity in binding. Moreover, unmodified nanoparticles did not show any binding to the two cell lines. Interestingly, it has also been demonstrated that SA-MIPs could specifically target cancer cells over normal cells, and that the addition of SA could compete out the SA-MIP binding to the cancer cells [26,34]. These results support our observations using the SA-derivatives, although we cannot completely reduce the binding to SA-expressing cells.

The majority of breast cancers carry Tn (GalNAc-Ser/Thr) within the same cell and in close proximity to extended glycan T (GalB1,3GalNAc), the addition of Gal to the GalNAc being catalyzed by the T synthase [35]. In breast cancer, there can also be a change in the number of O-GalNAc glycans added to the peptide core of glycoproteins, as well as changes in the core structures, which often results in increased sialylation. The sialylated derivatives of the O-GalNAc glycans are commonly observed, giving the sialylated Tn (STn) and sialylated core 1 (ST) glycans [29]. Truncated mucin-type O-linked glycans areseen often terminating in SA due to the up-regulation of sialyltransferases in breast cancers. The altered expression of the sialyltransferase is believed to be the main STn synthase [36]. However, novel diagnostic tools with better affinity and specificity are

needed. It has been shown that more than 90% of isolated CTC metastatic bladder and colorectal cancers can overexpress the STn antigen, which is significantly higher than EpCAM-based detection [37]. Recently, Kaptan et al. presented the effect of α-2,3 and α-2,6 on the cell proliferation, survival, and malignant behaviors of thyroid cancer cells. The authors treated the cancer cells with different plant lectins such as MALII, SNA, and Aleuria aurantia lectin (AAL) [38]. These results suggest that altered cell surface glycosylation in cancer seems to be a strong candidate for new therapeutic strategies.

In this study, we provide a discovery strategy in breast cancer cell lines to understand the binding pattern of lectins and MIPs targeting SA.

5. Conclusions

SA expression correlates with EpCAM and inversely with CD44 expression levels on a collection of breast cancer cell lines. SA expression could be detected, both with SA-MIPs and the lectins MAL I and SNA. Most interestingly, two different SA-derivatives used for the first time in this type of assay could significantly reduce the binding of the SA-MIPs in a concentration-dependent manner. This indicates that the SA-MIP binding to cells is mediated by direct interaction with SA. Indeed, we show that the SA-MIPs can function as an additional tool for detecting EpCAM-positive breast cancer cells. In conclusion, we show a combination of potential diagnostic cancer biomarkers that can be used to detect breast epithelial tumor cells that express SA. Further studies using cells from other tissue, including skin and colon, will reveal even novel SA-MIP staining patterns.

References

1. Howlander, N.; Noone, A.; Krapcho, M. SEER Cancer Statistics Review (CSR) 1975–2016. National Cancer Institute Website. Available online: https://seer.cancer.gov/csr/1975_2016/ (accessed on 15 December 2019).
2. Holliday, D.L.; Speirs, V. Choosing the right cell line for breast cancer research. *Breast Cancer Res.* **2011**, *13*, 215. [CrossRef]
3. Perou, C.M.; Jeffrey, S.S.; Van De Rijn, M.; Rees, C.A.; Eisen, M.B.; Ross, D.T.; Pergamenschikov, A.; Williams, C.F.; Zhu, S.X.; Lee, J.C. Distinctive gene expression patterns in human mammary epithelial cells and breast cancers. *Proc. Natl. Acad. Sci. USA* **1999**, *96*, 9212–9217. [CrossRef]
4. Zhu, Y.; Liu, R.; Huang, H.; Zhu, Q. Vinblastine-Loaded Nanoparticles with Enhanced Tumor-Targeting Efficiency and Decreasing Toxicity: Developed by One-Step Molecular Imprinting Process. *Mol. Pharm.* **2019**, *16*, 2675–2689. [CrossRef]
5. Pecot, C.V.; Bischoff, F.Z.; Mayer, J.A.; Wong, K.L.; Pham, T.; Bottsford-Miller, J.; Stone, R.L.; Lin, Y.G.; Jaladurgam, P.; Roh, J.W.; et al. A novel platform for detection of CK$^+$ and CK$^-$ CTCs. *Cancer Discov.* **2011**, *1*, 580–586. [CrossRef]
6. Van der Gun, B.T.F.; Melchers, L.J.; Ruiters, M.H.J.; de Leij, L.F.M.H.; McLaughlin, P.M.J.; Rots, M.G. EpCAM in carcinogenesis: The good, the bad or the ugly. *Carcinogenesis* **2010**, *31*, 1913–1921. [CrossRef] [PubMed]

7. Varki, A.; Lowe, J.B. Biological Roles of Glycans. In *Essentials of Glycobiology*, 2nd ed.; Varki, A., Cummings, R.D., Esko, J.D., Freeze, H.H., Stanley, P., Bertozzi, C.R., Hart, G.W., Etzler, M.E., Eds.; The Consortium of Glycobiology: La Jolla, CA, USA; Cold Spring Harbor, NY, USA, 2009.

8. Stowell, S.R.; Ju, T.; Cummings, R.D. Protein glycosylation in cancer. *Annu. Rev. Pathol.* **2015**, *10*, 473–510. [CrossRef]

9. Ulloa, F.; Real, F.X. Differential distribution of sialic acid in alpha2,3 and alpha2,6 linkages in the apical membrane of cultured epithelial cells and tissues. *J. Histochem. Cytochem.* **2001**, *49*, 501–510. [CrossRef]

10. Bogenrieder, T.; Herlyn, M. Axis of evil: Molecular mechanisms of cancer metastasis. *Oncogene* **2003**, *22*, 6524–6536. [CrossRef] [PubMed]

11. Büll, C.; Stoel, M.A.; den Brok, M.H.; Adema, G.J. Sialic acids sweeten a tumor's life. *Cancer Res.* **2014**, *74*, 3199–3204. [CrossRef] [PubMed]

12. Swindall, A.F.; Londono-Joshi, A.I.; Schultz, M.J.; Fineberg, N.; Buchsbaum, D.J.; Bellis, S.L. ST6Gal-I protein expression is upregulated in human epithelial tumors and correlates with stem cell markers in normal tissues and colon cancer cell lines. *Cancer Res.* **2013**, *73*, 2368–2378. [CrossRef] [PubMed]

13. Harduin-Lepers, A.; Krzewinski-Recchi, M.A.; Colomb, F.; Foulquier, F.; Groux-Degroote, S.; Delannoy, P. Sialyltransferases functions in cancers. *Front. Biosci.* **2012**, *4*, 499–515. [CrossRef]

14. Loureiro, L.R.; Carrascal, M.A.; Barbas, A.; Ramalho, J.S.; Novo, C.; Delannoy, P.; Videira, P.A. Challenges in antibody development against Tn and Sialyl-Tn antigens. *Biomolecules* **2015**, *5*, 1783–1809. [CrossRef] [PubMed]

15. El-Schich, Z.; Zhang, Y.; Feith, M.; Beyer, S.; Sternbæk, L.; Ohlsson, L.; Stollenwerk, M.; Wingren, A.G. Molecularly imprinted polymers in biological applications. *BioTechniques* **2020**, *69*, 406–419. [CrossRef] [PubMed]

16. Haupt, K.; Medina Rangel, P.X.; Bui, B.T.S. Molecularly imprinted polymers: Antibody mimics for Bioimaging and therapy. *Chem. Rev.* **2020**, *120*, 9554–9582. [CrossRef]

17. Piletsky, S.; Canfarotta, F.; Poma, A.; Bossi, A.M.; Piletsky, S. Molecularly imprinted polymers for cell recognition. *Trends Biotechnol.* **2020**, *38*, 368–387. [CrossRef] [PubMed]

18. Wulff, G. Molecular imprinting in cross-linked materials with the aid of molecular templates—a way towards artificial antibodies. *Angew. Chem. Int. Ed. Engl.* **1995**, *34*, 1812–1832. [CrossRef]

19. Wulff, G.; Sarhan, A.; Zabrocki, K. Enzyme-analogue built polymers and their use for the resolution of racemates. *Tetrahedron Lett.* **1973**, *14*, 4329–4332. [CrossRef]

20. Shinde, S.; El-Schich, Z.; Malakpour, A.; Wan, W.; Dizeyi, N.; Mohammadi, R.; Rurack, K.; Gjorloff Wingren, A.; Sellergren, B. Sialic Acid-Imprinted Fluorescent Core-Shell Particles for Selective Labeling of Cell Surface Glycans. *J. Am. Chem. Soc.* **2015**, *137*, 13908–13912. [CrossRef]

21. El-Schich, Z.; Abdullah, M.; Shinde, S.; Dizeyi, N.; Rosén, A.; Sellergren, B.; Wingren, A.G. Different expression levels of glycans on leukemic cells-a novel screening method with molecularly imprinted polymers (MIP) targeting sialic acid. *Tumor Biol.* **2016**, *37*, 13763–13768. [CrossRef]

22. Panagiotopoulou, M.; Kunath, S.; Medina-Rangel, P.X.; Haupt, K.; Bui, B.T.S. Fluorescent molecularly imprinted polymers as plastic antibodies for selective labeling and imaging of hyaluronan and sialic acid on fixed and living cells. *Biosens. Bioelectron.* **2017**, *88*, 85–93. [CrossRef]

23. Bie, Z.; Chen, Y.; Ye, J.; Wang, S.; Liu, Z. Boronate-affinity glycan-oriented surface imprinting: A new strategy to mimic lectins for the recognition of an intact glycoprotein and its characteristic fragments. *Angew. Chem. Int. Ed.* **2015**, *54*, 10211–10215. [CrossRef] [PubMed]

24. Xing, R.; Wang, S.; Bie, Z.; He, H.; Liu, Z. Preparation of molecularly imprinted polymers specific to glycoproteins, glycans and monosaccharides via boronate affinity controllable–oriented surface imprinting. *Nat. Protoc.* **2017**, *12*, 964–987. [CrossRef] [PubMed]

25. Liu, R.; Cui, Q.; Wang, C.; Wang, X.; Yang, Y.; Li, L. Preparation of sialic acid-imprinted fluorescent conjugated nanoparticles and their application for targeted cancer cell imaging. *ACS Appl. Mater. Interfaces* **2017**, *9*, 3006–3015. [CrossRef]

26. Wang, S.; Yin, D.; Wang, W.; Shen, X.; Zhu, J.-J.; Chen, H.-Y.; Liu, Z. Targeting and imaging of cancer cells via monosaccharide-imprinted fluorescent nanoparticles. *Sci. Rep.* **2016**, *6*, 22757. [CrossRef] [PubMed]

27. Panagiotopoulou, M.; Salinas, Y.; Beyazit, S.; Kunath, S.; Duma, L.; Prost, E.; Mayes, A.G.; Resmini, M.; Tse Sum Bui, B.; Haupt, K. Molecularly Imprinted Polymer Coated Quantum Dots for Multiplexed Cell Targeting and Imaging. *Angew. Chem. Int. Ed. Engl.* **2016**, *55*, 8244–8248. [CrossRef] [PubMed]

28. Johansson, E.; Caraballo, R.; Mistry, N.; Zocher, G.; Qian, W.; Andersson, C.D.; Hurdiss, D.L.; Chandra, N.; Thompson, R.; Frängsmyr, L. Pentavalent Sialic Acid Conjugates Block Coxsackievirus A24 Variant and Human Adenovirus Type 37–Viruses That Cause Highly Contagious Eye Infections. *ACS Chem. Biol.* **2020**, *26*, 2683–2691. [CrossRef]

29. Burchell, J.M.; Beatson, R.; Graham, R.; Taylor-Papadimitriou, J.; Tajadura-Ortega, V. O-linked mucin-type glycosylation in breast cancer. *Biochem. Soc. Trans.* **2018**, *46*, 779–788. [CrossRef]

30. Liu, X.; Yang, L.; Zhang, D.; Liu, T.; Yan, Q.; Yang, X. Deglycosylation of epithelial cell adhesion molecule affects epithelial to mesenchymal transition in breast cancer cells. *J. Cell. Physiol.* **2019**, *234*, 4504–4514. [CrossRef]

31. Kölbl, A.; Jeschke, U.; Andergassen, U. The significance of epithelial-to-mesenchymal transition for circulating tumor cells. *Int. J. Mol. Sci.* **2016**, *17*, 1308. [CrossRef]

32. Baccelli, I.; Schneeweiss, A.; Riethdorf, S.; Stenzinger, A.; Schillert, A.; Vogel, V.; Klein, C.; Saini, M.; Bäuerle, T.; Wallwiener, M. Identification of a population of blood circulating tumor cells from breast cancer patients that initiates metastasis in a xenograft assay. *Nat. Biotechnol.* **2013**, *31*, 539. [CrossRef]

33. Jing, X.; Cui, X.; Liang, H.; Hao, C.; Yang, Z.; Li, X.; Yang, X.; Han, C. CD24 is a potential biomarker for prognosis in human breast carcinoma. *Cell. Physiol. Biochem.* **2018**, *48*, 111–119. [CrossRef] [PubMed]

34. Yin, D.; Wang, S.; He, Y.; Liu, J.; Zhou, M.; Ouyang, J.; Liu, B.; Chen, H.-Y.; Liu, Z. Surface-enhanced Raman scattering imaging of cancer cells and tissues via sialic acid-imprinted nanotags. *Chem. Commun.* **2015**, *51*, 17696–17699. [CrossRef] [PubMed]

35. Beatson, R.; Maurstad, G.; Picco, G.; Arulappu, A.; Coleman, J.; Wandell, H.H.; Clausen, H.; Mandel, U.; Taylor-Papadimitriou, J.; Sletmoen, M. The breast cancer-associated glycoforms of MUC1, MUC1-Tn and sialyl-Tn, are expressed in COSMC wild-type cells and bind the C-type lectin MGL. *PLoS ONE* **2015**, *10*, e0125994. [CrossRef]

36. Marcos, N.T.; Bennett, E.P.; Gomes, J.; Magalhaes, A.; Gomes, C.; David, L.; Dar, I.; Jeanneau, C.; DeFrees, S.; Krustrup, D. ST6GalNAc-I controls expression of sialyl-Tn antigen in gastrointestinal tissues. *Front. Biosci.* **2011**, *3*, 1443–1455. [CrossRef]

37. Neves, A.A.; Stockmann, H.; Harmston, R.R.; Pryor, H.J.; Alam, I.S.; Ireland-Zecchini, H.; Lewis, D.Y.; Lyons, S.K.; Leeper, F.J.; Brindle, K.M. Imaging sialylated tumor cell glycans in vivo. *FASEB J. Off. Publ. Fed. Am. Soc. Exp. Biol.* **2011**, *25*, 2528–2537. [CrossRef]

38. Kaptan, E.; Sancar-Bas, S.; Sancakli, A.; Bektas, S.; Bolkent, S. The effect of plant lectins on the survival and malignant behaviors of thyroid cancer cells. *J. Cell. Biochem.* **2018**, *119*, 6274–6287. [CrossRef] [PubMed]